RSC Advances

ROYAL SOCIETY OF CHEMISTRY

www.rsc.org/advances

Cite this: DOI: 10.1039/c0xx00000x

www.rsc.org/xxxxxx

ARTICLE TYPE

Towards implantable porous silicon biosensors

Leandro N. Acquaroli,[a] Tim Kuchel[b] and Nicolas H. Voelcker*[a]

Received (in XXX, XXX) XthXXXXXXXXX 20XX, Accepted Xth XXXXXXXXX 20XX
DOI: 10.1039/b000000x

Porous silicon (pSi) is a nanomaterial with salient properties for optical biosensor applications. For example, the material displays strong and tunable optical reflectance is highly biocompatible and biodegradable. The material is compatible with microfabrication and can be produced in the form of films, membranes and particles. Whilst pSi has been used extensively as a biosensor to accept analytes in or purified from body fluids, it has never been used as an implantable biosensor. In this paper, we advance the understanding of the requirements for pSi-based optical biosensors when incorporated under skin. Reflectance spectra from several different pSi thin film architectures were compared. The optical properties of pSi films were optimised and pSi microcavities with resonances at 850 nm were found to be the most suitable for implantable biosensors. This work will provide useful cues for researchers interested in developing implantable biosensors for human medical and veterinary applications.

Introduction

Porous silicon (pSi) is a nanostructured material, which continues to rouse broad interest in the materials science community due to its unique optical, electronic and biomaterials properties. These properties have underpinned a variety of applications from opto-electronic devices to biosensors and scaffolds for stem cells [1-5].

The properties of pSi such as its large surface area (up to 800 m^2/g), its fast preparation and its diverse and tuneable optical and surface-chemical properties have predestined this material for sensor and biosensor applications [3,6-12]. Porous silicon films of several micrometer thicknesses formed on crystalline Si by electrochemical etching are subject to thin film interferences when illuminated with either white light from a conventional lamp, or by illuminating with a laser [1,2,6,13]. This optical effect can be detected with a charge-coupled detector (CCD) spectrometer as Fabry-Perot fringes, which contain information about the effective refractive index of the porous layer (n) and the thickness of the layer (d). A change in the refractive index of the porous layer (e.g. upon binding of biological macromolecules inside the pores) manifests itself in a shift of the fringe pattern and a corresponding change in the effective optical thickness of the layer (defined as the product of n times d) [1,2,6,13]. By varying the current density during the etching process, pSi can assume double- or multilayered structures. Alternating between two distinct currents in real time results in discrete modulations in porosity and hence in refractive index with depth in a stepwise fashion. This gives rise to Bragg reflectors in which only light at a defined wavelength corresponding to the photonic bandgap is reflected [1,2,14,15]. In rugate filters, which are obtained by the sinusoidal variation of the current density, sidelobes seen in Bragg reflectors are reduced and cleaner resonances are produced [16]. On the downside, peak reflectance is reduced [17,18]. Microcavities are 1D photonic bandgap structures that include a spacer layer positioned between two Bragg reflectors resulting in the formation of a narrow photonic resonance, which appears as a dip in the reflectance spectrum and is highly sensitive to changes in refractive index [6], such as those arising from binding of biomolecules in the pores [7,19].

Porous silicon is remarkably inert and non-inflammatory within the body and has been investigated as a biomaterial in the form of films, membranes and particles, including nanoparticles [20-24]. The main advantage over other biomaterials lies in its ability to degrade completely in aqueous solutions into non-toxic silicic acid, the major bioavailable form of silicon in the human body [25]. The structural integrity of the material can be preserved and the degradation kinetics controlled from hours to months by modifying the surface using silanisation, hydrosilylation and thermal carbonisation [26]. Porous silicon has been used as a scaffold for the attachment, growth and recently even transfer of mammalian cells including stem cells and as a platform for drug delivery [20,27].

Even though pSi is a biocompatible biosensor material, to the best of our knowledge no reports are currently available on implanted pSi biosensors. In this work, we investigate various pSi reflectors for their ability to produce reflectance signals when placed underneath cadaver skin. This study provides fundamental understanding that is required for the design of implantable optical biosensors. Potential target applications for these biosensors include the monitoring of changes in hormone levels which relate to endocrine diseases including diabetes, thyroid, pituitary or sex hormone disorders.

Experimental details

Fabrication of porous silicon thin films

Porous silicon thin films with single layers, rugate filters and

microcavities configurations were fabricated using a computer controlled Keithley 2425 source meter. Samples were prepared by electrochemical anodisation of p-type boron doped crystalline silicon (c-Si) wafers (5 mΩ·cm, resistivity and <100> orientation), in a 1 HF : 2 EtOH (v/v) solution, at room temperature. For each film, the initial pSi parasitical layer was removed using a 1 M solution of sodium hydroxide [7], and then the etching of the final layers were carried out.

Current densities between 90 to 160 mA·cm^{-2}, for etching times from 200 to 700 s, were used to fabricate pSi single layers. In order to characterise pSi single layers, the absolute reflectance of each fabricated sample was measured and fitted using conventional algorithms, transfer matrix method and the effective medium theory proposed by Looyenga [14]. From this fitting procedure, porosity and thickness of each pSi film were obtained. In order to prepare pSi microcavities, two different current densities were chosen with their respective etching rates and porosities, characterised from pSi single layers method. Then, quarter wavelength layers [28] were designed, and fabricated at different wavelengths in order to obtain different optical responses for the microcavities. pSi-based rugate filters were fabricated following reference [17], with an average current density 85 mA·cm^{-2} and etching times values of 340 and 450 s.

For improved chemical stability in aqueous environment, freshly etched pSi films were oxidised during 1 h under ozone ambient, at room temperature, employing an ozone generator [6].

Preparation of cadaver skins

Rabbit and guinea pig skins provided by the Large Animal Research and Imaging Facility (SAHMRI, located in Adelaide, Australia) were utilised in the experiment. These samples were collected from animals used in other experiments with approval from the SA Pathology Animal Ethics Committee. Full thickness pieces of skin samples (2 x 2 cm^2) were stored in saline solution inside a fridge at 4 ºC. The hair and the fat layer of the skins were removed using a scalpel before optical measurements, so as to reduce the scattering and absorption of light. The thicknesses of the skins were measured with a micrometer, and their values vary around 1 ± 0.05 mm for the guinea pig skin, and 2 ± 0.1 mm for the rabbit skin. It is worth noting that the skin thicknesses used in this work, are in the order of that of dermis in human skin [29]. Glycerol at 87% and a saturated sucrose solution were used as optical clearing agents for different skins samples. Skins were incubated in these two solutions at room temperature throughout experiments.

Reflectance measurements through skin

Optical reflectance measurements through different animal skins were carried out using a LS-1 tungsten halogen light source and an USB4000 Ocean Optics spectrometer in the visible range. A scheme of the experimental setup is shown in Figure 1, where the skin is placed on the top surface of the pSi thin film. Reflection spectra through skins were taken in two different solutions, glycerol and sucrose.

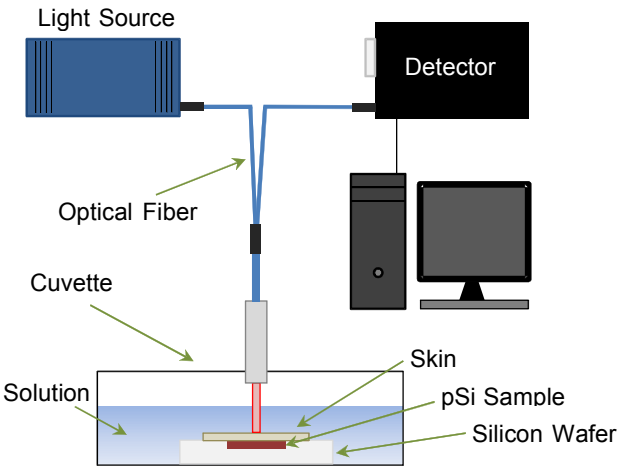

Fig. 1 *Scheme of the experimental setup for the reflection measurements of pSi reflectors through animal cadaver skin.*

Results and discussion

Since cadaver skin rapidly turns opaque, optical measurements of skin-embedded pSi reflectors were performed in glycerol and sucrose solution. This will simulate the situation in a living animal. These solutions reduce scattering and absorption of animal and human skin, avoid dehydration and provide refractive index matching [29-33].

Reflection spectra for pSi single layer films, microcavities and rugate filters placed underneath guinea pig and rabbit skin are presented in Figure 2. The time evolution of the reflection spectra for distinct pSi thin films is shown in each graph after immersion in glycerol (Figure 2a-f). Spectra in Figure 2a, 2c, 2e and 2g correspond to pSi samples placed underneath rabbit skin, whereas Figure 2b, 2d, 2f and 2h show spectra from pSi reflectors underneath guinea pig skin. From Figure 2, it is possible to observe that cadaver skin scattering can be overcome by immersion of the reflector-skin assembly in either glycerol or sucrose solution. For rabbit skin, 24 h treatment was required to obtain high-quality reflectance spectra whereas for guinea pig skin, 3 h immersion in glycerol was sufficient. One simple explanation may be that the rabbit skin used is thicker than guinea pig skin, so the index matching solution needs more time to take effect [29]. Alternatively, glycerol might interact differently on the two animal skin types due to the different texture and composition, and this also could lead to the observed discrepancy.

Measurements of reflection with skin immersed in sucrose solution were also performed. No optical signal could be obtained after 24 h of immersion of the reflector-skin assemblies (Figure 2g-h). This result was surprising since sucrose solution has been used successfully for the purpose of refractive index matching of mice cadaver skin [29].

Cite this: DOI: 10.1039/c0xx00000x

www.rsc.org/xxxxxx

ARTICLE TYPE

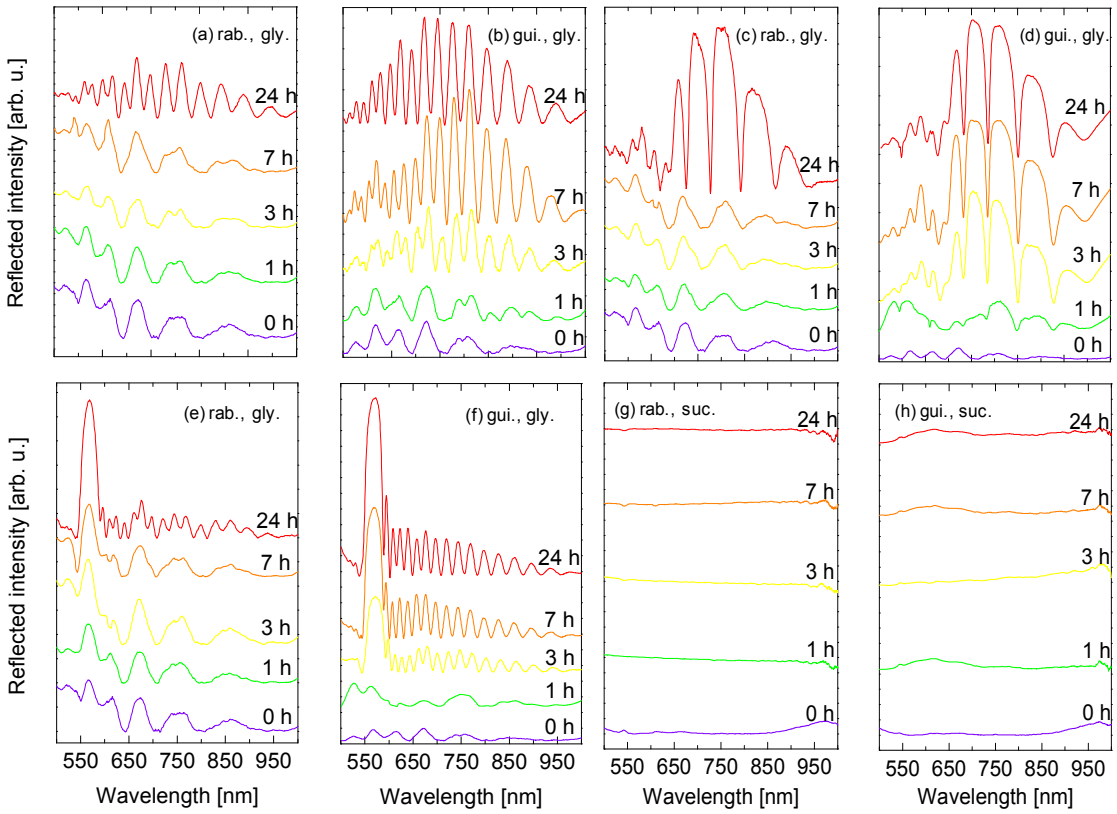

Fig. 2 Evolution of reflection spectra over a period of 24 h for rabbit skin (a, c, e, g) and guinea pig skin (b, d, f, h) skins in glycerol (a-f) and sucrose (g, h) solution. (a, b, g, h) correspond to a pSi single layer, (c, d) pSi microcavity, (e, f) pSi rugate filter, respectively. In the legends, gui., rab., gly., and suc., stand for guinea, rabbit, glycerol and sucrose, respectively.

According to these results, and especially those for guinea pig skin in glycerol solution, optical signals from pSi reflectors can be readily read out through the skins, and processed either by Fourier transforming single layers spectra, or by following the peak of the narrow filter-like spectral features of multilayer pSi structures. Although animal skin was used in this work, glycerol has been previously used as an index matching fluid for human skin as optical clearing agent for improvement of laser tattoo removal from the body [32]. Our results therefore set the stage for the development of pSi based implantable biosensors which take advantage of the optical properties and the good biocompatibility and biodegradability of pSi. Furthermore, pSi reflectors can be fabricated in the form of membranes or microparticles which can be easily implanted or even injected underneath the skin. If the readout occurs through an optical fiber, a geometric sample area of less than 0.5 mm2 is required. The ease of this approach has significant advantages in comparison to the highly complex optical scattering methods and microscopy described somewhere else [29,33-35]. Another advantage of the method employed here is that no optically toxic chromophores or fluorophores are required for biological detection [36,37].

The reflection spectra taken in the above experiments cover the wavelength range from 500 nm to 1000 nm, in agreement to the so-called optical window in biological tissue [38]. By controlling the fabrication conditions for pSi, it is possible to tune the optical response within this window. Our results suggest that pSi based implantable biosensors could be implemented over a broad wavelength range, potentially allowing multiplexing of implantable biosensors.

In Figure 3, pictures of pSi thin films are shown either covered with rabbit skin and guinea pig skins using either glycerol of sucrose for index matching. Figure 3a presents a pSi reflector underneath hairless guinea pig skin at time zero of incubation (without incubation of the skin in solution) in glycerol. At this point, the skin is so opaque that it is difficult to see the pSi reflector underneath. Figure 3b shows two different pSi thin films in glycerol solution, which were used in the following pictures, covered by guinea pig and rabbit skins. In Figures 3c and 3e, the same pSi sample covered by guinea pig (c) and rabbit (e) skins are shown, while in Figures 3d and 3f, the other pSi sample covered by guinea pig and rabbit skins, respectively, are observed. The characteristic colors of pSi thin films are clearly visible through the skin, in agreement to reflection spectra shown in Figure 2.

In Figure 3g, another set of pSi samples incubated in sucrose solution are shown without cadaver skin cover, while in Figure 3h, these same samples covered by guinea pig (left) and rabbit (right) skins are depicted after 24 h incubation.

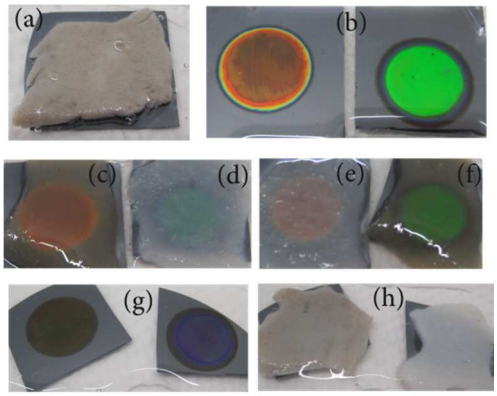

Fig. 3 Photographs of pSi reflectors covered by skin samples. (a) Guinea pig skin onto pSi sample before incubation of skin (zero time) in glycerol. (b) pSi samples in glycerol solution. (c and f) Guinea pig skin samples on different pSi reflectors shown in (b) after 24 h incubation in glycerol. (d and e) Rabbit skin samples on both pSi reflectors shown in (b) after 24 h incubation in glycerol. (g) Exemplar pSi reflectors in sucrose solution. (h) Guinea pig (left) and rabbit (right) skins onto pSi reflectors of (g) after 24 h treatment in sucrose.

We then obtained further proof that pSi reflectors underneath skin samples can be optically interrogated. A single layer with the same conditions to the one used to measure the spectra in Figure 2b was fabricated for this purpose. The reflectance spectrum of the freshly etched sample in air was taken and fitted using the matrix method theory along with the Looyenga effective medium theory, obtaining a thickness of 3530 nm and a porosity of 70%. Using this pSi sample, we measured the reflected intensity when immersed in glycerol solution with and without cadaver skin on top.

Taking the Fast Fourier Transform to both intensity spectra, the mean effective optical thicknesses obtained were 7200 nm and 7370 nm, respectively. Using Looyenga effective medium theory, the refractive index of glycerol [39], the value of the porosity and the effective optical thickness, we calculated the thickness of the sample: 3520 nm for the FFT measurement without skin and 3560 nm for the FFT measurement with the skin on top, both in glycerol solution. These results are consistent with the thickness calculated from the measurements of the freshly etched sample, confirming the idea that the main interference pattern fringes result from the solution/pSi/c-Si interfaces. Differences in the exact values are a consequence of the fabrication method and can be explained in terms of small radial variations in pSi film thickness.

Having demonstrated the ability to obtain optical signals from pSi films through animal skin, we next step determined the most suitable wavelength band for this work. In order to optimise the wavelength, four pSi microcavities showing resonances at different wavelengths across the optical window were prepared and tested underneath skin samples in glycerol. pSi microcavities were chosen among the different pSi architectures. Due to the sharp and narrow resonances in their optical spectra, they are more suitable to detect very small changes of refractive indexes than compared to rugate filters and Bragg mirrors, by [6-11].

Figure 4 shows the reflection spectra of four pSi microcavities centered at four different positions across the optical window. For each microcavity, the quality factor (Q, given as the central wavelength of the resonance divided by the full width at half maximum [28]) was calculated. As seen from Figure 4, the Q factor of the samples immersed in glycerol increased, for increasing central wavelength of the resonance from 550 nm (a), 650 nm (b), 750 nm (b) to 850 nm (d), with Q values 110, 126, 146 and 176, respectively. Owing to the high absorption of silicon in the short wavelength region [1,2], microcavities present a better shape when they are centered at higher wavelengths. The resonance shift after immersion in glycerol is due to the increase in the refractive index inside the pores.

After the microcavities were characterised, they were placed under guinea pig skin and the evolution of the reflection spectra of these samples for different incubation times in glycerol studied. The results are shown in Figure 5 and confirm the earlier results that 3 h immersion in glycerol is sufficient to obtain transparency but improvements in signals were achieved up to 24 h. In order to determine which microcavity was best suited for implanted biosensor applications, the Q factors of the four pSi microcavities fabricated were assessed and compared. It can be seen from the data that the best Q factors were obtained for microcavities centered about 750 and 850 nm. Since the Q factor measures how far a microcavity is from the ideal condition (microcavity with a delta shape resonance) due to light absorption and other dissipation mechanisms [28], these results indicate that skin (after treatment with glycerol for 24 h) is transparent over the analyzed wavelength range, and that the optical quality of the microcavity is mainly subject to the absorption spectrum of porous silicon.

The Q factors values for microcavities with resonances in 550 and 650 nm were about 12% and 13% lower, respectively, when measured with the cadaver skin on top (compare Figures 4a with 5a, and Figures 4b with 5b). On the contrary, the Q factors for the microcavities with resonances peaking at 750 and 850 nm, show only a small reduction (5% and 2%, respectively) in their values with the skin on top (compare Figures 4c with 5c, and Figures 4d with 5d). This can also be explained taking into account the low absorption and scattering mechanisms at longer wavelengths within the spectral range considered. However, if a particular sensing application requires a different working wavelength, shorter wavelength can be used, as shown in Figure 5b and 5c, where good Q factors are attainable still remains compared to those reflectors without skin (Figure 4).

This set of experiment provides design principles for pSi based optical biosensors implanted under the skin. Although glycerol-treated animal cadaver skin is somewhat different from living skin, the optical properties of glycerol-treated cadaver skin are similar to living skin and the results are expected to be transferrable [29,30]. In future work, we will carry out in vivo testing where we will implant the most suitable pSi reflector identified during the in vitro testing subcutaneously in a rodent. We will also need to address other issues related to the use of pSi reflectors for implantable biosensors including the effect of pSi degradation on the optical signal and the biocompatibility of the reflectors in vivo. Our previous work with regards to stabilising

the porous silicon surface chemistry and our previous in vivo biocompatibility testing give us confidence that these hurdles can be overcome [3,20].

Conclusions

We have explored the use of pSi thin films to read optical reflectance signals through animal cadaver skin. An assessment of the optical response of pSi thin films suggests that the addition of refractive index matching solutions on cadaver skin mimics the conditions of live animal skin and allows the acquisition of reflectance spectra. We demonstrated that prolonged incubation of tissues in glycerol improved the quality of the reflectance spectra through both rabbit and guinea pig skin, with

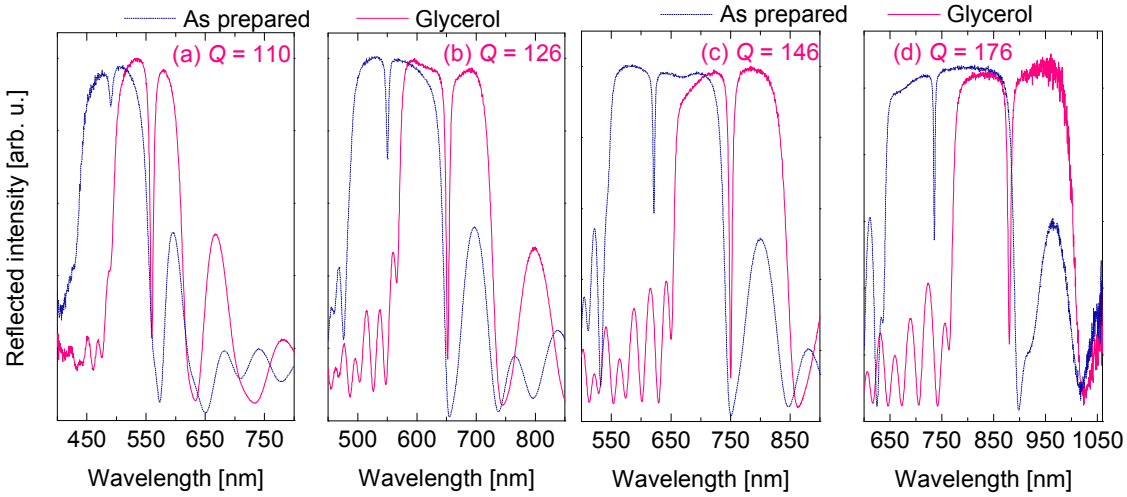

Fig. 4 Reflection spectra of pSi microcavities with the microcavity resonances centered at four different wavelengths in air and immersed in glycerol. The corresponding Q factor is depicted in each graph, for the spectra of pSi measured in glycerol solution (the horizontal axis changes in each figure, but the size of the spectral window was kept constant for comparison).

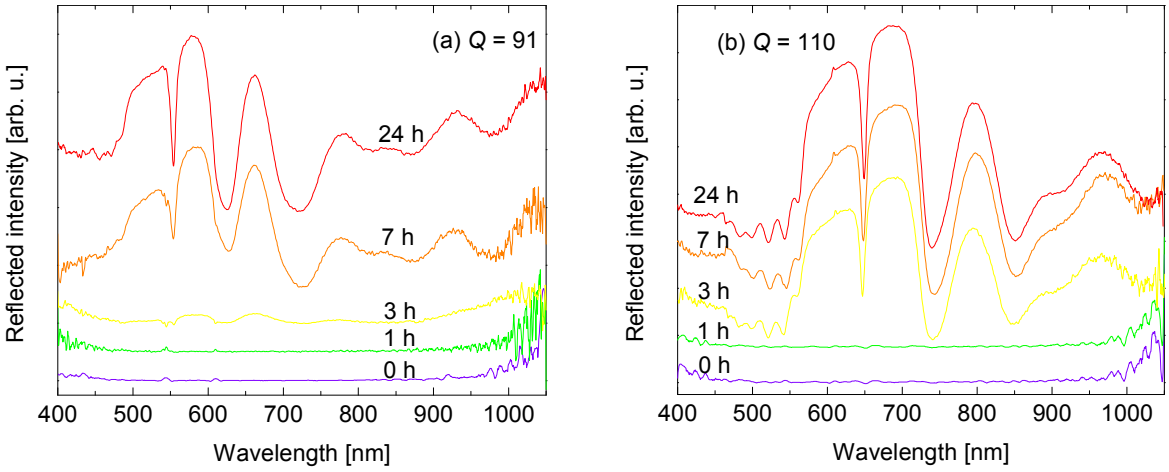

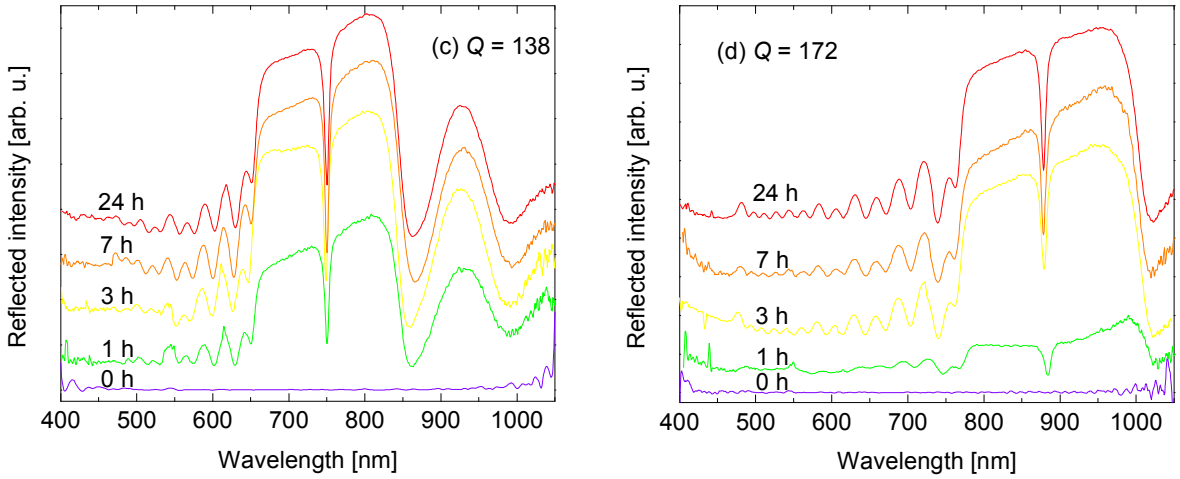

Fig.5 Evolution of reflection spectra of the four pSi microcavities described in Figure 4 covered by guinea pig skin upon immersion in for different times. The Q factor is presented in each plot, for 24 h immersion time.

the latter skin type affording higher quality spectra. We also showed through the study of the evolution of reflection spectra that porous silicon microcavities could be employed as integrated devices in implants under skins, with the best result obtained for photonic structures with the main resonance centered at 850 nm. Our work paves the road for the development of pSi biosensors implanted subcutaneously in the form of membranes or particles and a read-out through the skin using an external reflectance probe. This technology will have wide-spread applications for the management of human diseases and in particular endocrine disorders.

Notes and references

[a]*Mawson Institute, University of South Australia, GPO Box 2471, Adelaide SA 5001, Australia. Fax: +61 8 83025613; Tel: +61 8 83703221; E-mail: nico.voelcker@unisa.edu.au*
[b]*South Australian Health and Medical Research Institute, 101 Blacks Road, Gilles Plains SA 5086, Australia.*

† Electronic Supplementary Information (ESI) available: [details of any supplementary information available should be included here]. See DOI: 10.1039/b000000x/

1 O. Bisi, S. Ossicini and L. Pavesi. *Surface Science Reports*, 2000, **38**, 1.
2 W. Theiß. *Surface Science Reports*, 1997, **29**, 91.
3 S. P. Low, N. H. Voelcker, L. T. Canham and K. A. Williams. *Biomaterials*, 2009, **30**, 2873.
4 A. Bragaru,M. Kusko,M. Simion, A. Iordanescu, R. Pascu,B. M. Danila, F. Craciunoiu and M. Diaconu. *Semiconductor Conference (CAS)*, 2011, **1**, 117.
5 S. M. Haidary, E. P. Córcoles and N. K. Ali. *Journal of Nanomaterials*, 2012, **2012**, 830503.
6 L. N. Acquaroli, R. Urteaga and R. R. Koropecki. *Sensors and Actuators B: Chemical*, 2010, **149**, 189.
7 H. Ouyang, M. Christophersen, R. Viard, B. L. Miller and P. M. Fauchet. *Advanced Functional Materials*, 2005, **15**, 1851.
8 S. Chan, P. M. Fauchet, Y. Li, L. J. Rothberg and B. L. Miller. *Physica Status Solidi (a)*, 2000, **182**, 541.
9 V. Mulloni and L. Pavesi. *Applied Physics Letters*, 2000, **76**, 2523.
10 S. Chan, Y. Li, L. J. Rothberg, B. L. Miller and P. M. Fauchet. *Materials Science and Engineering: C*, 2001, **15**, 277.
11 L. De Stefano, I. Rendina, L. Moretti, S. Tundo and A. M. Rossi. *Applied Optics*, 2004, **43**, 167.
12 A. Jane, R. Dronov, A. Hodges and N. H. Voelcker. *Trends in Biotechnology*,2009, **27**, 230.
13 L. N. Acquaroli, R. Urteaga, C. L. A. Berli and R. R. Koropecki. *Langmuir*, 2011, **27**, 2067.
14 L. N. Acquaroli. *Propiedades ópticas de silicio poroso nanoestructurado*. Tesis Doctoral, 2011. Argentina.
15 Y. L. Khung and N.H. Voelcker. *Optical Materials*, 2009, **32**, 234.
16 M. Sweetman and N. H. Voelcker.*RSC Advances*, 2012, **2**, 4620.
17 E. Lorenzo, C. J. Oton, N. E. Capuj, M. Ghulinyan, D. Navarro-Urrios, Z. Gaburro and L. Pavesi. *Applied Optics*, 2005, **44**, 5415.
18 E. Lorenzo, C. J. Oton, N. E. Capuj, M. Ghulinyan, D. Navarro-Urrios, Z. Gaburro and L. Pavesi. *Physica Status Solidi (c)*,2005, **2**,227.
19 F. Vollmer, D. Braun, A. Libchaber, M. Khoshsima, I. Teraoka and S. Arnold. *Applied Physics Letters*, 2002,**80**, 4057.
20 S. P. Low, K. A. Williams, L. T. Canham and N. H. Voelcker. *Biomaterials*,2006, **27**, 4538.
21 E. J. Anglin, L. Cheng, W. R. Freeman and M. J. Sailor. *Adv Drug Deliv Rev*. 2008,**60**, 1266.
22 L. T. Canham, C. L. Reeves, A. Loni, M. R. Houlton, J. P. Newey, A. J. Simons and T. I. Cox. *Thin Solid Films*, 1997, **297**, 304.
23 L. T. Canham. *Adv. Mater*. 1995, **7**, 1033.
24 Y.L. Khung, G. Barritt and N. H. Voelcker. *Experimental Cell Research*,2008, **314**, 789.
25 J.-H. Park, L. Gu, G. von Maltzahn, E. Ruoslahti, S. N. Bhatia and M. J. Sailor. *Nature Materials*,2009, **8**, 331.
26 H. A. Santos, J. Riikonen, J. Salonen, E. Mäkilä, T. Heikkilä, T. Laaksonen, L. Peltonen, V.-P. Lehto and J. Hirvonen. *Acta Biomaterialia*,2010, **6**,2721.
27 E. Secret, K. Smith, V. Dubljevic, E. Moore, P. Macardle, B. Delalat, M.-L. Rogers, T. G. Johns, J.-O. Durand, F. Cuninand N. H. Voelcker. *Adv. Healthcare Mat.*, 2013, **2**, 626.
28 A. V. Kavokin, J. J. Baumberg, G. Malpuech and F. P. Laussy. Microcavities. Oxford University Press, New York, 1st. Ed., 2007.
29A. N. Bashkatov, E. A. Genina, I. V. Korovina, Y. P. Sinichkin, O. V. Novikova, and V. V. Tuchin. *Proc. SPIE 4241, Saratov Fall Meeting 2000: Optical Technologies in Biophysics and Medicine II*, 2001, **2001**, 223.
30 K. Moulton, F. Lovell, E.Williams, P. Ryan, D. C. Lay, Jr., D. Jansen and S. Willard. *Journal of Biomedical Optics*, 2006, **11**, 052027.
31 O. Stumpp, B. Chen and A. J. Welch. *Journal of Biomedical Optics*, 2006, 11, 041118.
32 E. A. Genina, A. N. Bashkatov, A. A. Gavrilova, A. B. Pravdin, V. V. Tuchin, I. V. Yaroslavsky and G. B. Altshuler. *Proc. SPIE 6734, International Conference on Lasers, Applications, and Technologies 2007: Laser Technologies for Medicine*, 2007, **2007**, 673419.
33 R. Cicchi, D. Sampson, D.Massi and F. Pavone. *Optics Express*, 2005, **13**, 2337.

34 S. B. Bambot, G. Ra, M. Romauld, G. M. Carter, J. Sipior, E. Terpetchnig and J. R. Lakowicz. *Biosensors & Bioelectronics*, 1995, **10**, 643.
35 A. N. Bashkatov, E. A. Genina and V. V. Tuchin. *Journal of Innovative Optical Health Sciences*,2011, **4**, 9.
36 J.-H. Park, A. M. Derfus, E. Segal, K. S. Vecchio, S. N. Bhatia and M. J. Sailor. *J. Am. Chem. Soc.*, 2006, **128**, 7938.
37 G. Palestino, V. Agarwal, R. Aulombard, E. Perez and C. Gergely. *Langmuir*, 2008, **24**, 13765.
38 L. V. Wang and H. Wu. Biomedical optics: Principles and Imaging. Wiley, 1st Ed., 2007.
39 J. Rheims, J. Köser and T. Wriedt. *Meas. Sci. Technol.*,1997, **8**, 601.